LA-UR -82-2528

Conf-820942--1

LA-UR--82-2528

DE82 021694

TITLE: APPLICATION OF NUCLEAR MODELS TO NEUTRON NUCLEAR CROSS SECTION CALCULATIONS

AUTHOR(S): Phill[illegible] G. Young, T-2

SUBMITTED TO: The Nuclear Data for Science and Technology International Conference, Antwerp, Belgium, 6-10 September 1982

Los Alamos National Laboratory
Los Alamos, New Mexico 87545

FORM NO. 836 R4
ST. NO. 2629 5/81

APPLICATION OF NUCLEAR MODELS TO NEUTRON NUCLEAR CROSS SECTION CALCULATIONS

Phillip G. Young

Theoretical Division, Los Alamos National Laboratory
Los Alamos, New Mexico 87545 U.S.A.

Nuclear theory is used increasingly to supplement and extend the nuclear data base that is available for applied studies. Areas where theoretical calculations are most important include the determination of neutron cross sections for unstable fission products and transactinide nuclei in fission reactor or nuclear waste calculations and for meeting the extensive dosimetry, activation, and neutronic data needs associated with fusion reactor development, especially for neutron energies above 14 MeV. Considerable progress has been made in the use of nuclear models for data evaluation and, particularly, in the methods used to derive physically meaningful parameters for model calculations. Theoretical studies frequently involve use of spherical and deformed optical models, Hauser-Feshbach statistical theory, preequilibrium theory, direct-reaction theory, and often make use of gamma-ray strength function models and phenomenological (or microscopic) level density prescriptions. The development, application, and limitations of nuclear models for data evaluation are discussed in this paper, with emphasis on the 0.1 to 50 MeV energy range.

[Nuclear reaction theory, nuclear model codes, nuclear data evaluation]

Introduction

Requirements for nuclear data are sufficiently broad that even with our present body of experimental data many areas remain where the application of nuclear theory is important. The purposes for applying theory range from providing simple interpolation tools in regions where measurements are abundant and consistent to actually predicting nuclear data for nuclei or energy regions inaccessible to experiment. The most common situation involves both these extremes in that one usually builds a theoretical parameter base from the available experimental data and then uses theory to extrapolate that information into unknown regions. The uncertainty in the final result depends, of course, upon how "far" the extrapolation is in a physical sense.

The most stringent predictive requirements for theory involve such applications as neutron absorption and scattering by reactor fission products; production, depletion, and absorption calculations for actinides produced in reactors; dosimetry and activation calculations for unstable nuclides that will be produced in fusion reactors; and extension of the data base to the 15 to 50 MeV energy range for facilities that utilize higher energy neutrons, for example, d + Li neutron sources. It should be emphasized, however, that the application of theory for evaluation purposes remains important even for the more common materials where measurements are abundant. The reason is simply that discrepancies occur in the experimental data base, and nuclear theory can provide hints both as to whether in fact discrepancies exist in given situations and what the resolution of the discrepancies might be.

The aim of this paper is to briefly review the main nuclear reaction models that are being used to calculate data for applications and to convey an idea of their capabilities and deficiencies. To avoid redundancy with other papers, only applications of theory above $E_n \sim 100$ keV will be discussed and fission will not be considered. Emphasis will be given to the general features of the theories, as several excellent papers are available that detail the mathematics (for example, see Refs. 1-7).

We will begin with a brief discussion of theory applications for light elements, but most of the paper will focus on analyses of neutron-induced reactions on intermediate and heavy mass materials involving spherical or deformed optical models, preequilibrium theory, and Hauser-Feshbach statistical theory. Some of the nuclear theory computer codes in common use will be summarized, and example calculations [illegible] described. We will conclude by briefly discussing some of the directions being pursued that offer promise for improved predictions in the future.

Applications of Theory for Light Elements

Because of the individual character of most light elements, the use of nuclear theory in developing applied data has been mainly limited to short extrapolations of experimental data using fairly simple models. An important exception to this occurs for coupled-channel R-matrix theory, which has been extensively applied in several light element systems, particularly the A = 7 and 11 systems that include the ^{6}Li(n,α) and ^{10}B(n,α) standard reactions.[8,9] Other compound systems where R-matrix methods have been used are A = 2, 3, 4, 5, 13, 16, and 17.[10]

In conjunction with the R-matrix studies, a new resonance model has recently been developed by Hale[11] to describe energy spectra of particles in reactions involving three-body final states. Typically, such spectra consist of relatively narrow peaks on top of broad, underlying structures commonly attributed to "three body phase space" contributions. However, such structures can also come from kinematically broadened resonance effects. In the new model, an expression for the transition amplitude was derived from the three-body Schroedinger equation, assuming that the relative wave functions for pairs of final-state particles are dominated by single resonances. This assumption allows the three-body spectra to be calculated in terms of known parameters for the two-body resonances, with full account being taken of interference between direct and exchange amplitudes.

Calculations of the neutron emission spectra with 14.1-MeV incident neutrons are compared in Fig. 1 to measurements[12] at 10 and 60° and to other calculations.[13] There is reasonable agreement in shape at both angles (note that the calculated curves have not been broadened for experimental resolution), but the 60° calculation overpredicts the data somewhat. This model is still under development, but it offers promise to broaden the scope of several R-matrix-based evaluations for light elements.

Other areas where nuclear theory is utilized for light element applications include use of optical, statistical, and intranuclear-cascade models to extrapolate data to unmeasured regions. For example, a spherical optical model fit of elastic angular distributions below 15 MeV and total cross sections from 10 to 20 MeV was recently used[14] to extrapolate a ^{7}Li evaluation to 20 MeV. Similarly, intranuclear-cascade

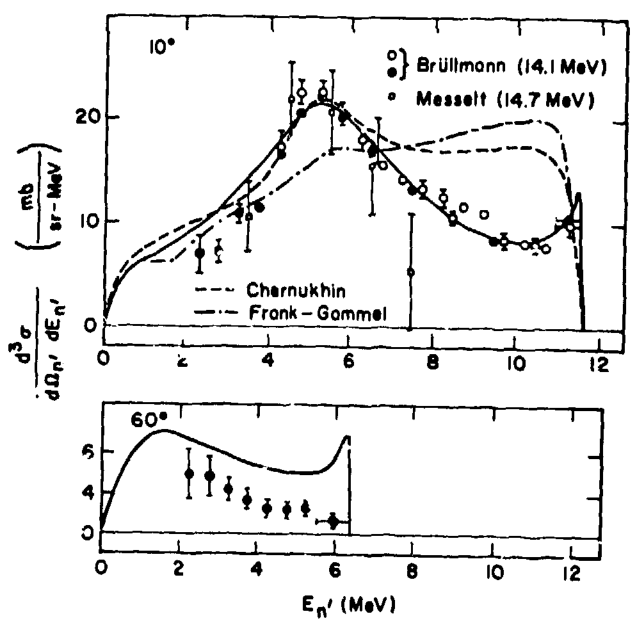

Fig. 1. Resonance model calculations (solid curves) compared to measured[12] n + d neutron spectra at θ_{lab} = 10 and 60° for 14.1-MeV incident neutrons. The dashed curves represent other calculations.[13]

ments of hydrogen and helium emission spectra from 27 to 61 MeV neutron reactions on carbon to develop a data base for several applications in this region.

Intermediate- and Heavy-Mass Nuclei

The sequence of steps followed in applying nuclear theory for data evaluation of intermediate- or heavy-mass nuclei can vary greatly depending on the nuclei involved, the energy range and reaction types required, and the accuracy needed in the evaluation. Typically, an analysis involves determination of optical model potentials for both neutrons and charged particles; development of a model for calculating gamma-ray transmission coefficients; use of a level density formulation in combination with the available experimental data on discrete states; estimation of direct and preequilibrium reaction effects; use of a fission model when appropriate; and specification of a framework for combining the above components, usually Hauser-Feshbach statistical theory. More advanced unified theories[16-18] that combine compound and direct reaction effects in a realistic manner are being explored in nuclear data calculations[18-20] but have thus far not seen wide use in applied data calculations. This approach is the subject of other papers[21,22] at this conference and will not be discussed here.

Optical Model Analyses

Most modern theoretical data evaluations are built around an optical-model analysis using either a spherical or deformed potential, depending upon the particular mass region being studied. The importance of this component to an analysis is obvious since it provides not only the total, shape elastic, and reaction cross sections but also the neutron and charged-particle transmission coefficients that are used in Hauser-Feshbach statistical theory calculations. An important and demanding requirement of such analyses is that they usually must cover a very wide energy range; typically, 1 keV to 20 MeV or higher. The low-energy transmission coefficients continue to be important even for high incident energies in order to correctly calculate particle emission in the various reaction chains.

Except for general scoping calculations or studies in regions completely devoid of data, the modern trend is to focus such analyses on the mass region of immediate interest rather than to use global optical model parameters. The SPRT method developed by Lagrange[23] and coworkers has been widely used to determine optical model parameters. Basically, this method involves fitting experimental values of s- and p-wave neutron strengths, potential scattering radius, total cross sections, and elastic and inelastic scattering data to determine the optical model parameters. Automated fitting techniques are generally not required with this method but have frequently been used[24-26] in determining spherical potentials.

Computations with deformed optical potentials are much more time consuming, of course, and one of the advantages of the SPRT method has been that automatic searching is not required. It has been observed in several analyses[24-26] that calculated (n,xn) cross sections near threshold are very sensitive to low energy transmission coefficients, and comparisons with experiment have been used to test or further optimize parameters determined by the SPRT approach.

An important development that significantly reduces computation time in deformed optical model analyses for odd-A nuclei is described in a recent paper by Lagrange, Bersillon, and Madland.[27] Using a strong coupling rotational model, it is shown that coupled-channel calculations for an odd-A nucleus can be approximated by performing the same calculation with a suitably chosen (fictitious) K = 0 rotational band and appropriately combining the results. For example, calculations for the ground-state rotational band of ^{239}Pu coupling 5-states (J = 1/2, 3/2, ..., 9/2) can be accurately approximated by a 3-state calculation (J = 0, 2, 4) with a reduction by a factor of 27 in computing time. Similarly, replacement of a ^{241}Pu calculation coupling 5-states having J = 5/2, 7/2, ..., 13/2 by an appropriate J = 0, 2, 4 calculation reduces computation time by a factor of ~ 54, although the approximation is poorer.

A comparison of cross sections calculated at E_n = 4 MeV for the above cases is given in Table I. The approximation is nearly exact for ^{239}Pu (K = 1/2) at this energy. The fictitious values are less precise for ^{241}Pu (K = 5/2) but note that the integrated cross sections are still quite accurate. Although not shown, similar accuracies are achieved for transmission coefficients after suitable collapsing.

Even using such approximate methods, the complexity and expense involved in performing coupled-channel calculations when many levels are involved quickly becomes prohibitive. Hodgson[28] recently proposed an alternative method for calculating inelastic cross sections. In particular, he determined that, if the coupling between excited states is small, inelastic scattering can be calculated for deformed nuclei with standard DWBA theory but using a deformed potential to determine the exit channel wave function.

Increasing emphasis has been placed in recent years on linking analyses of (n,n), (p,p), and (n,p) data by means of the Lane model.[29] Basically, this model relates the nuclear potentials for the three different reaction types through isospin considerations and permits, for example, the deduction of neutron potentials from the analysis of proton measurements. Recent reviews discussing and applying this model have been given by Rapaport[30] and by Hansen.[31] The latter review also addresses the importance of including coupling effects in calculations of deformed nuclei, and both topics are illustrated in Fig. 2, taken from that paper.

Figure 2 compares calculations of (n,n) scattering angular distributions with measurements[32] for Ta, Au,

Table I Comparison of ^{239}Pu (K=1/2) and ^{241}Pu (K=5/2) Cross Sections Using Real and Fictitious Levels in Coupled-Channel Calculations for 4-MeV Neutrons.
(σ_i refers to the cross sections of the first four excited states.)

	^{239}Pu		^{241}Pu	
	Real	Fictitious	Real	Fictitious
σ_{TOT}	7.797 b	7.796 b	7.821 b	7.831 b
σ_{CN}	3.124	3.124	3.171	3.120
σ_{EL}	4.249	4.247	4.343	4.398
σ_1	0.1233	0.1232	0.1533	0.1660
σ_2	0.1845	0.1847	0.0864	0.0751
σ_3	0.0[illegible]2	0.0517	0.0418	0.0674
σ_4	0.0644	0.0646	0.0268	0.0117

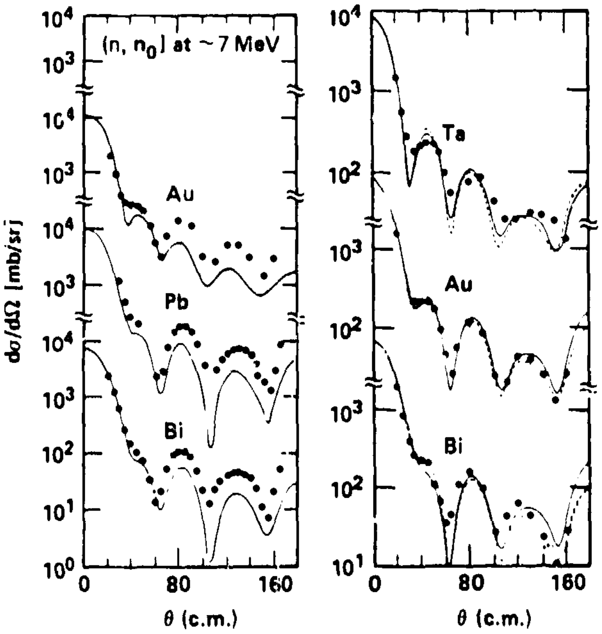

Fig. 2. Calculated and measured[32] neutron elastic measurements near 7 MeV as presented in Ref. 31 See text for details.

Pb, and Bi near 7 MeV. The neutron potential used to calculate the solid curves on both sides of the figure were determined using the Lane model from analyses of (p,p) and (p,n) data. The curves on the left were obtained in a distorted-wave Born approximation (DWBA) calculation,[33] whereas the ones on the right result from a coupled-channel calculation.[34] The coupled-channel calculations using the Lane formalism agree about as well with the (n,n) experiments as do calculations using neutron global parameters[35] (optimized to fit neutron data), shown by the dashed curves. The agreement with experiment is much poorer for the DWBA calculations.

Other developments that hold promise for improved predictive capabilities are the efforts at several laboratories to integrate microscopic model calculations into determination of optical potentials. Starting from basic calculations by Jeukenne, Lejeune, and Mahaux[36] of the optical potential in nuclear matter, Lagrange and Brient[37] have performed microscopic calculations of elastic and inelastic scattering from ^{208}Pb in the 8.5-61 MeV energy range. Similarly, Dietrich et al[38] found reasonable agreement with 24-MeV neutron scattering data for ^{208}Pb in a microscopic folding model calculation. Microscopic calculations have also been

Gamma-Ray Transmission Coefficients

In a recent review of fast neutron capture calculations. Gardner[3] summarized the status of statistical, direct, and semidirect theories used in calculations. A qualitative view of the relative importance of these contributions to (n,γ) cross sections is given in Fig. 3. For orientation, the rapid falloff of the statistical contribution typically occurs near E_n = 1 MeV, and the peak in the semidirect contribution is in the neighborhood of 14 MeV, where the (n,γ) cross section is ~ 1 mb. For most applications the statistical contribution is clearly the most important of the three.

Two models are commonly used to determine gamma-ray transmission coefficients for statistical calculations, the Weisskopf single-particle model[39] and the giant dipole resonance (GDR) model.[40] Of these, the GDR model has been most successful in reproducing gamma-ray strength functions inferred from experimental data. Normalization of the gamma-ray strength function $f(E_\gamma)$ is usually accomplished from experimental information on $<\Gamma_\gamma>$ and $<D_o>$, the average gamma-ray width and spacing for s-wave resonances, through the relation

$$\frac{2\pi<\Gamma_\gamma>}{<D_o>} = \int_0^{S_n} f(E_\gamma)E_\gamma^3\ \rho\ (S_n-E_\gamma)dE \quad , \qquad (1)$$

where S_n is the neutron binding energy and ρ is the level density of the compound system.

The strength function for electric dipole radiation, which is the dominant transition, is usually taken as Lorentzian in shape (or as a sum of 2 Lorentzians for deformed nuclei). More recently Gardner et al[3,41] have investigated the use of Breit-Wigner shapes and have developed expressions for f_{E1} based on systematics covering the mass range A < 40. A comparison of strength functions calculated with both representations is given in Fig. 4 with points inferred from measurements[42] on ^{89}Y. While the normalizations of both curves are somewhat high in this case, the shape of the dashed curve calculated using the Breit-Wigner form more nearly follows the measured points. In most applied problems where f_{E1} is used to compute capture cross sections or gamma-ray competition with particle emission, the results are not highly sensitive to this difference in shape, and the Lorentzian is still commonly used.

The preferred method[43] for performing gamma-ray calculations in regions where $<\Gamma_\gamma>$ or $<D_o>$ in Eq. (1) are unmeasured is to extrapolate the strength function f_{E1} rather than $<\Gamma_\gamma>$ and $<D_o>$. The latter quantities can vary by orders of magnitude in nearby nuclei, making reliable extrapolation difficult, whereas f_{E1} changes much more slowly.

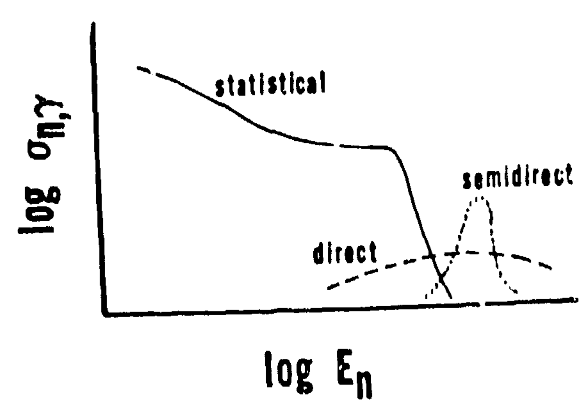

Fig. 3. Schematic view of the relative importance of different reaction mechanisms [illegible]

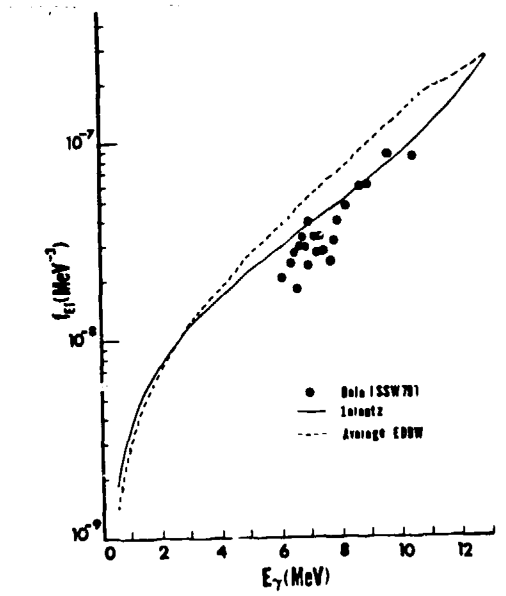

Fig. 4. Comparison of experimental values[35] of $f_{E1}(E_\gamma)$ from n + ^{89}Y with calculations using the Lorentz form and the Breit-Wigner (EDBW) form.

Nuclear Level Densities

The Hauser-Feshbach expression for the cross section from the initial state C to the final state C' through the compound nucleus spin and parity $J\pi$ is[44]

$$\sigma^{J\pi}_{CC''} = \frac{\langle\Gamma^{J\pi}_{C}\rangle \langle\Gamma_{C'}\rangle^{J\pi}}{\langle\Gamma^{J\pi}\rangle} W^{J\pi}_{CC'} \qquad (2)$$

where $W^{J\pi}_{CC'}$ is a width-fluctuation correction[4] important at lower energies but which approaches one above a few MeV. The partial widths are obtained by summing the particle or gamma-ray transmission coefficients over the possible transitions to levels in the final state. Because level spacings rapidly become very small as excitation energy is increased, a continuum of levels must be introduced and the density of such levels specified.

For reasons of convenience, most calculations of applied data employ phenomenological level density models. The most commonly used are the Gilbert and Cameron[45] and back-shifted Fermi-gas models,[46] as well as a model by Ignatuyk[47] that has seen extensive use in (n,2n) calculations[48]. The Gilbert and Cameron model consists of a constant temperature form at low excitation energies, which is smoothly joined to a Fermi-gas shape at higher excitation energies. The level density parameters (a and T) are determined from empirical s-wave level spacings at the neutron binding energy (E_x ~ 6 MeV) and from matching with the available discrete level data at low excitation energies. The back-shifted Fermi-gas model is a little simpler, consisting of a pure Fermi gas form. Its variables involve a level density parameter, a, and a ground-state energy-shift parameter, Δ, which are determined from the same data described above. The Ignatuyk expressions incorporate an excitation-energy dependent level-density parameter. Recent improvements to these models include a more accurate specification of spin cutoff parameters by Reffo[49] and updated fits by Cook[50] of other parameters.

Phenomenological level density parameters are determined mainly near the neutron binding energy, and the energy dependence of shell and pairing effects is not necessarily well represented. Microscopic calculations of the state density, on the other hand, incorporate shell effects naturally because they use realistic shell-model single-particle levels, and the effects.[51] More recently, improved formalisms have been developed to handle unpaired nucleons in odd-A systems, that is, to include the blocking effect of single-particle levels due to the unpaired nucleon.[52] While such microscopic models are not necessarily more accurate at present than the phenomenological ones, they do include improved physics and are expected to better predict the energy dependence of level densities away from regions of experimental data.

A comparison of the Gilbert and Cameron and the back-shifted Fermi-gas phenomenological models with a microscopic thermodynamic model[53] was presented by Arthur[7] and is expanded in Fig. 5. In the upper half of the figure the state densities for ^{238}U calculated with the microscopic model are plotted versus excitation energy. In the lower half, the ratios of the Gilbert and Cameron and the back-shifted Fermi-gas models to the microscopic model are shown, with all the calculations normalized to experiment at the neutron binding energy (~ 6.1 MeV). No attempt was made to optimize the phenomological model parameters to represent the microscopic calculation; they were simply taken from the literature.[46,54]

The state densities from the phenomenological level densities differ from the microscopic calculation by as much as a factor of 2 between E_x = 0 and the neutron binding energy and by even greater factors at higher excitation energies. The region between E_x = 1 and 5 MeV is particularly important for calculating (n,n'), (n,xn), and (n,f) reactions. Although some cancellation of errors in level densities can occur in calculating competing reactions, this area is probably the one most in need of improvements for applied calculations.

Statistical-Preequilibrium Theory

For incident neutron energies above about 10 MeV, statistical model calculations of neutron cross sections and spectra must be corrected for nonequilibrium effects. The master equation exciton model[55] has been widely used in evaluations to calculate preequilibrium particle emission, as has the geometry-dependent hybrid model.[56] The basic idea of the master equation exciton model is that a given reaction is assumed to proceed through a series of particle-hole configurations, starting with simple ones and proceeding through more complicated ones until equilibrium is reached. At each stage during the process, particle

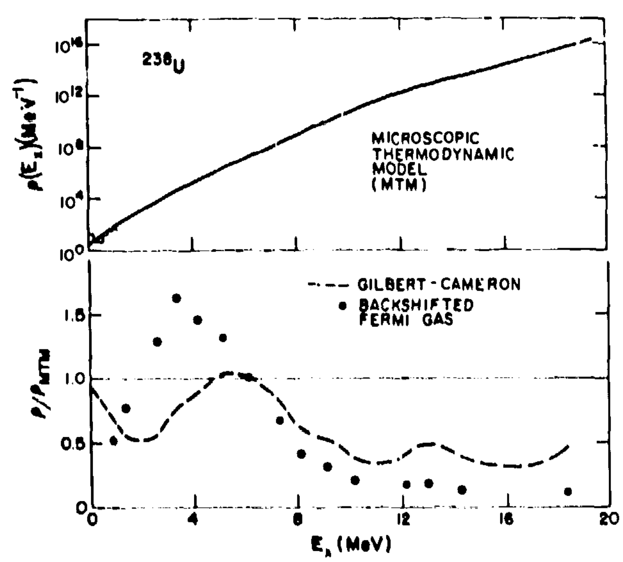

Fig. 5. Comparison of state densities calculated using a microscopic thermodynamic model[53] with values from the Gilbert and Cameron[45] and back-shifted Fermi-gas[46] models.

emission can occur with some probability, and a series of coupled equations must be solved to obtain cross sections and spectra.

Several recent reviews[6] address preequilibrium theory in some detail. In his review, John considers the merits of both the master equation and geometry-dependent hybrid approaches and includes a number of example calculations. He points out that the latter model depends only on optical model parameters and takes into account the diffuseness of the nuclear surface.

In other developments, Akkermans et al[57] have developed a unified model of equilibrium and preequilibrium emission, still based on the master equation, that permits calculation of angular distribution effects. The results are found to agree reasonably up to an outgoing energy of about 30 MeV with the semiempirical formulation of Kalbach and Mann,[58] which is commonly used in data evaluations. Applying Monte Carlo techniques, Akkermans and Gruppelaar[59] have used this model to calculate preequilibrium effects for the second and third particles in a reaction chain. Their results indicate that inclusion of preequilibrium in the tertiary steps is unnecessary below 50 MeV but is important for second particle emission above 25 MeV.

A procedure commonly followed in statistical preequilibrium calculations that carry angular momentum effects is to simply correct or scale the energy dependence of cross sections for emitted particles to account for preequilibrium effects. The statistical spin distribution of states in the final nucleus is then still maintained and does not properly reflect the preequilibrium process. Fu[60] has developed a procedure for incorporating preequilibrium effects into the angular momentum distribution of final states. Such considerations might be important, for example, in calculating production cross sections for isomers created in (n,2n) reactions. Fu has recently used this procedure to calculate cross sections for specific gamma rays created in the $^{57}Fe(n,2n\gamma)^{56}Fe$ reaction.[61] Comparisons with a measurement at 15 MeV are shown in Table II.

Table II Comparisons of Calculated and Experimental $^{57}Fe(n,2n\gamma)^{56}Fe$ Gamma-Ray Cross Sections (mb) for $E_n \sim$ 15 MeV

Gamma-Ray Energy	Production Cross Section (mb) Predicted	Experiment
847	980	1071 ± 59
1238	425	451 ± 36
1811	39	33 ± 17
2113	36	41 ± 17
1038	46	61 ± 14
1303	73	117 ± 16
367	8	17 ± 6
1670	27	53 ± 11

Statistical-Preequilibrium Codes

A number of computer codes have been developed over the past few years that combine statistical and preequilibrium theory for the purpose of data evaluation. A selection of these are described here. See references 62 and 63 for more complete summaries.

The multireaction Hauser-Feshbach statistical preequilibrium codes GNASH,[64] HAUSER5,[65] STAPRE,[66] and TNG[67] have been used extensively over the past few years. All four codes include full allowance for angular momentum effects and can calculate particle spectra as well as cross sections. All except HAUSER output gamma-ray spectra, and all except GNASH include width fluctuation corrections. The TNG code calculates angular distributions including preequilibrium effects, whereas GNASH, HAUSER, and STAPRE depend upon external codes for angular effects. GNASH, HAUSER5, and STAPRE include fission channels with double-humped barriers and a similar capability is under development for TNG. GNASH and STAPRE are usually used in combination with the reaction theory code COMNUC[68] at lower energies. All four codes have been employed up to incident neutron and/or proton energies in the 30-50 MeV range. In addition to these codes, a more advanced multireaction Hauser-Feshbach code is under development by Uhl and Strohmaier that will automate much of the code setup and will be better adapted for evaluation work.[69]

The MSPQ[70] and ALICE[71] codes use evaporation theory for the statistical portion of the calculation and preequilibrium emission based on the master equation exciton and geometry-dependent hybrid models, respectively. Both codes calculate particle emission spectra, and MSPQ contains a fission channel as well.

The AMALTHEE[72] and PREANG[73] codes both use matrix methods to solve exactly the master equations of the exciton model without artificial division between preequilibrium and equilibrium components. PREANG has recently been modified to utilize a random walk model that simplifies and compacts calculations of multiparticle emission.[59] Both codes calculate particle emission spectra, and PREANG also calculates particle angular distributions.

Hauser-Feshbach Statistical-Preequilibrium Calculational Examples

There are a number of recent studies in which rather complete theoretical analyses have been performed in association with data evaluations. To illustrate the use of multireaction Hauser-Feshbach statistical preequilibrium calculations, some of the details of recently completed analyses of neutron reactions on ^{165}Ho, ^{169}Tm, and $^{182,183,184,186}W$ will be described. These analyses are linked through use of very similar deformed optical model parameterizations. Emphasis will be on the W-isotope analysis, as it preceeded the Ho and Tm work, and the latter analysis is described in detail in another paper at this conference.[74] Several other recent analyses will also be briefly summarized.

Ho-Tm-W Analysis

Earlier calculations for W-isotopes using a spherical optical potential are described in a paper at the 1979 Knoxville conference.[75] The difficulty and ambiguity associated with deriving an equivalent spherical optical potential to represent deformed nuclei over extended energy ranges motivated us to revise the analysis using a deformed optical potential.[76] This approach has the advantage that a single neutron potential is used to calculate total, shape elastic, and direct inelastic cross sections as well as the neutron transmission coefficients used in compound elastic, (n,γ), (n,n'), and (n,xn) reaction calculations. To illustrate the inadequacy of spherical potentials in this mass region, a comparison is given in Fig. 6 of total and nonelastic cross sections from our coupled-channel (CC) analysis and values calculated with the spherical potential of Moldauer,[77] which gives good agreement with data for A < 140.

We used a symmetric rotational model with coupling of the ground state band members in our analysis, even though there is evidence of mixing between the two lowest band members for ^{183}W and ^{186}W. For the even-even isotopes, we chose a 0^+, 2^+, 4^+ coupling basis, while for ^{183}W the equivalent $1/2^-$, $3/2^-$, $5/2^-$, $7/2^-$, $9/2^-$ basis was used.

The deformed optical potential was obtained by modifying the potential of Delaroche et al.[78] to obtain reasonable agreement with (n,2n) measurements on the four major W-isotopes near threshold. Care was taken to maintain the good agreement with W experimental data for s- and p-wave neutron strengths, potential scattering radii, neutron total cross sections to 15 MeV, (n,n) and (n,n') angular distributions at 3.4 MeV, and (p,p') angular distributions at 16 MeV that Delaroche had established in his SPRT analysis. Subsequently, the parameterization (with some modification) was found to give reasonable agreement with experimental data for ^{165}Ho and ^{169}Tm, as described in Ref. 74 and shown in Fig. 6 for σ_{TOTAL}(^{165}Ho). The calculation of the 3.4-MeV elastic and inelastic ^{184}W angular distribution and experimental data[78] are shown in Fig. 7, together with the ENDF/B-V evaluation (dashed curve).

The deformed optical model parameterization for W-isotopes from this analysis is given in Table III. The notation and form of the potential are the same as in Refs. 74 and 78. Slight modifications to the tabulated values of V and W_D were used in the actual evaluations to optimize agreement with data for the individual isotopes.

We obtained our gamma-ray transmission coefficients from an empirically determined gamma-ray strength function. A sum of two Lorentzians was used to represent f_{E1} [see Eq. (1)], with parameters taken from photonuclear measurements. The overall normalization of $f(E_\gamma)$ was achieved by comparison with (n,γ) cross-section measurements below 1 MeV for the various isotopes. Standard parameters were used for the exciton model preequilibrium calculation in the GNASH code, and level density parameters for the Gilbert and Cameron[45] formulation were obtained from the Cook tables.[54]

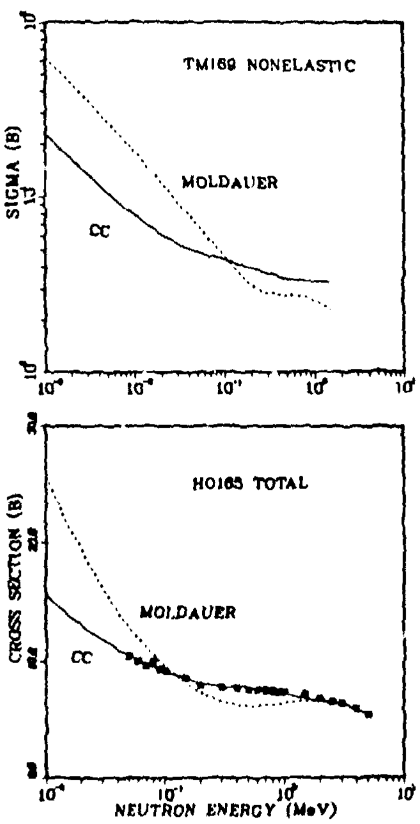

6. Comparison of ^{169}Tm nonelastic and ^{165}Ho
l cross sections calculated using a coupled-channel
ysis (Parameter Set 1 in Ref. 74) with values cal-
ted from a spherical optical potential.[77] The

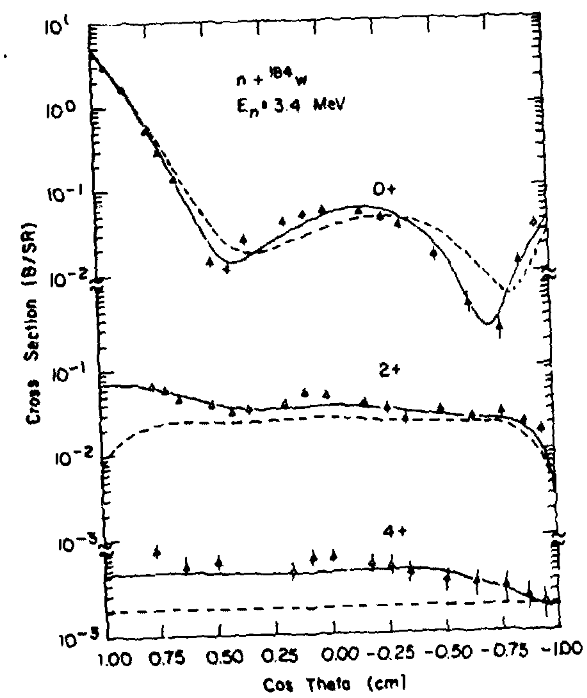

Fig. 7. Calculated[76] and measured[78] elastic and inelastic angular distributions for states in ^{184}W with 3.4-MeV incident neutrons. The dashed curves are ENDF/B-V.

Table III. Optical Parameters for Tungsten Isotopes

$$V\binom{n}{p} = 49.8\,(\mp)16\,\frac{N-Z}{A} + \Delta V_c - 0.25E$$

$$\Delta V_c = 0.4\,\frac{Z}{A^{1/3}} \qquad \text{for incident protons}$$

$$= 0 \qquad \text{for incident neutrons}$$

$$W_D\binom{n}{p} = 5.1\,(\mp)8\,\frac{N-Z}{A} + 0.6E \qquad [E \le 6.5]$$

$$= 9.0\,(\mp)8\,\frac{N-Z}{A} - 0.1(E-6.5) \qquad [E > 6.5]$$

$$W_V = -1.8 + 0.2\,E \qquad [E > 9.0]$$

$$V_{SO} = 7.5$$

$$r_V = r_{SO} = 1.26\text{f};\ r_d = 1.24\text{f}$$

$$a_V = a_{SO} = 0.61\text{f};\ a_D = 0.45\text{f}$$

Isotope	β_2	β_4
^{182}W	0.223	-0.054
^{183}W	0.220	-0.055
^{184}W	0.209	-0.056
^{186}W	0.195	-0.057

Comparisons of calculated values with a few of the experimental results that were not included in the analysis are given in Figs. 8-10. Figure 8 compares the calculations (solid curves) with measurements by Smith et al[79] of inelastic scattering excitation functons for four levels in ^{184}W (the 1/125-MeV "level" is actually a cluster of three levels). The upper curves are for the 2^+ and 4^+ levels, which contain substantial direct reaction contributions, whereas the lower curves are entirely compound-nucleus calculations. The dashed curves represent ENDF/B-V.

Figure 9 compares the composite neutron emission spectrum from calculation of the four isotopes with 14-MeV measurements[34] for natural tungsten. There is some disagreement among the various measurements, but the calculation seems to represent the mean rather well above ~ 1.5 MeV and agrees with Vonach's data at lowwre energies.

Figure 10 compares calculated gamma-ray emission spectra for natural tungsten with three measurements[32] near 7.4 MeV. There is significant disagreement for E_γ > 2 MeV with the Dickens data, but generally reasonable agreement with the other measurements. This trend is observed in similar comparisons at other energies and could indicate an experimental problem.

As an additional illustration of the predictive capability of such analyses, a comparison is shown in Fig. 11 of preliminary experimental data by Haouat and Patin[80] with results from the ^{165}Ho and ^{169}Tm analysis described in Ref. 74. Neutron scattering

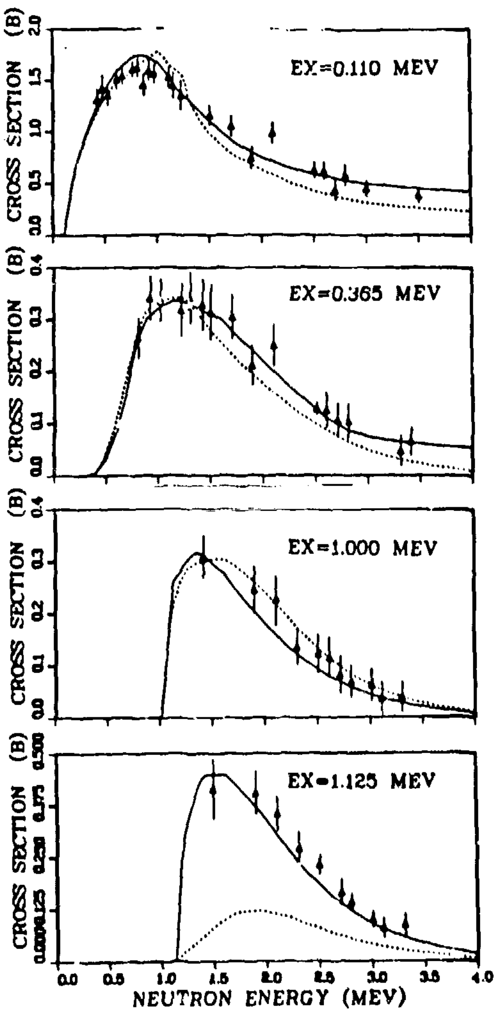

Fig. 8. Comparison of calculated[76] and measured[79] excitation functions for $^{184}W(n,n')$ reactions to four excited states. Th...

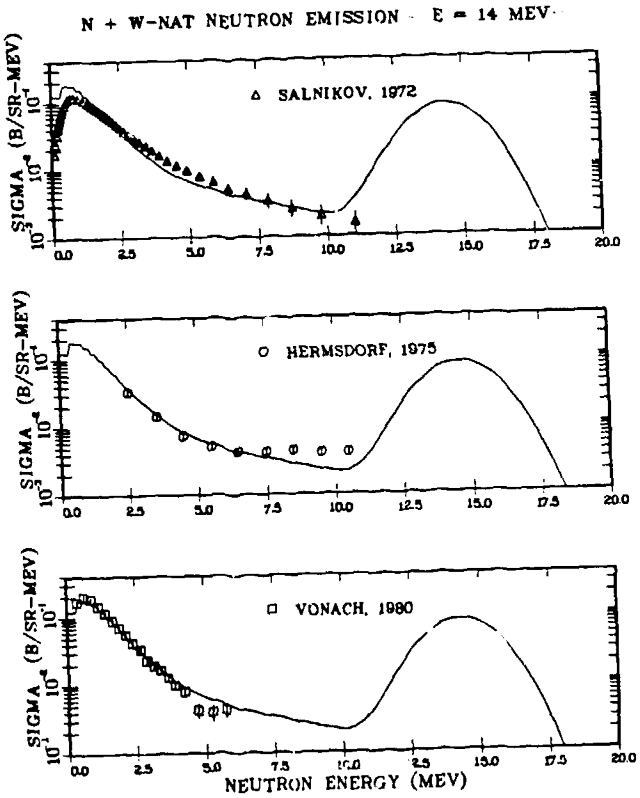

Fig. 9. Calculated[76] and measured[32] neutron emission spectra from 14-MeV neutron bombardment of natural W.

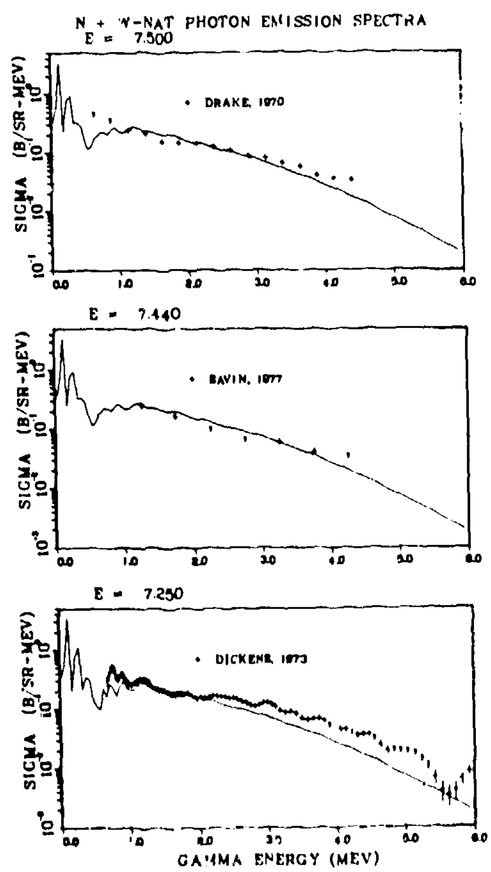

Fig. 10. Calculated[76] and measured[32] gamma-ray emission spectra from ~ 7-MeV neutron interactions on natural W.

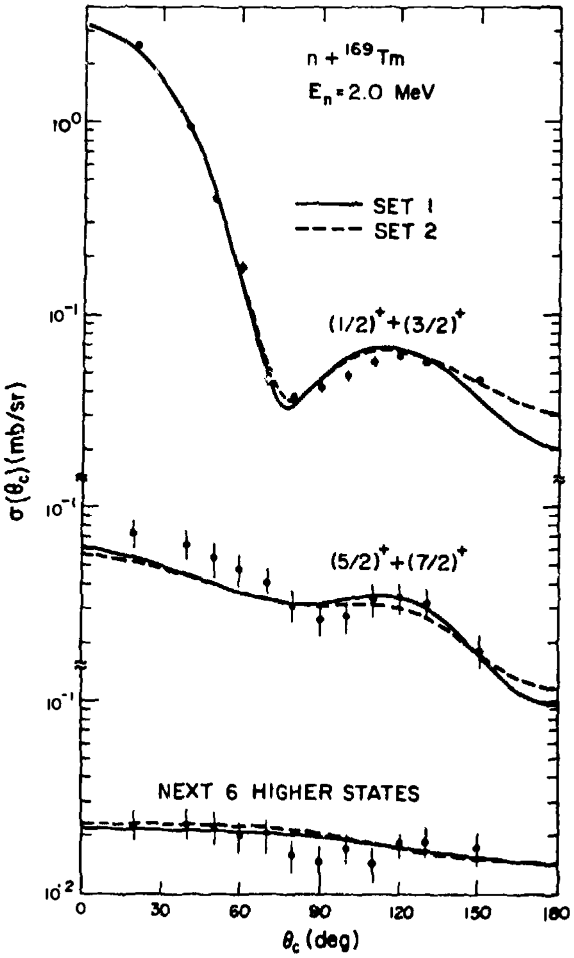

Fig. 11. Comparison of calculated elastic and inelastic neutron angular distributions at 2 MeV with the preliminary measurements of Haouat and Patin.[80] The solid and dashed curves represent coupled-channel calculations with Parameter Set 1 and Set 2 of Ref. 74.

data for ^{169}Tm were not available for that analysis, which mainly involved small modifications to the parameters of Table III to improve agreement with total cross-section data. The dashed curves represent the final results of that analysis.

Other Statistical-Preequilibrium Analyses

Other good examples of multireaction Hauser-Feshbach statistical-preequilibrium analyses include the papers at this conference by Strohmaier et al[81] describing an analysis of ^{52}Cr, ^{55}Mn, ^{56}Fe, and ^{58,60}Ni cross sections to 30 MeV with the STAPRE code; and an analysis using the COMNUC and GNASH codes of neutron data to 20 MeV for ^{209}Bi by Bersillon et al.[82] Both analyses utilize spherical optical potentials and use techniques similar to those described above.

The TNG code has recently been used by Fu[81] to update ENDF/B data for Fe and Cu, and by Hetrick et al[83] to calculate neutron-induced reactions on ^{40}Cu from 20 to 40 MeV. During the Cu analysis, a factor of 5 error was discovered in the ENDF/B-IV ^{63}Cu(n,p) cross section due to a misinterpretation of experimental data by the ENDF/B-IV evaluator. A comparison of calculated and experimental[84] proton emission spectra for 14-MeV neutrons on ^{63}Cu is shown in Fig. 12 with the individual reaction components separated. The error in ENDF/B-IV resulted because the (n,pn) reaction component of Fig. 12 was erroneously included in the (n,p) cross section. Fu's analysis[81] of Fe also supported an earlier observation by Young et al,[85] based on nuclear model calculations, that an error is likely in a 14-MeV measurement[86] of the gamma-ray emission spectrum from Fe.

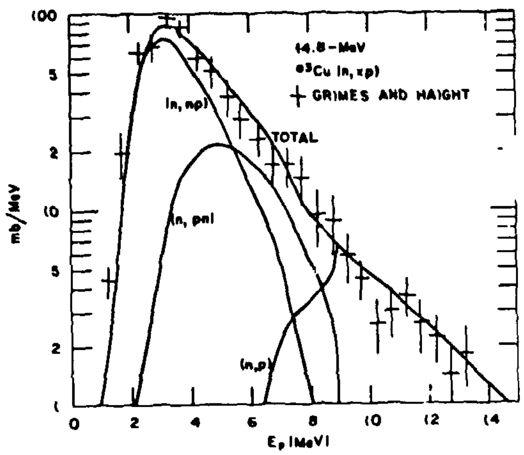

Fig. 12. Calculated[81] and measured[84] proton emission spectra from 14.8-MeV neutron bombardment of ^{63}Cu.

In the ^{40}Ca analysis by Hetrick et al,[83] experimental total cross sections and elastic angular distributions for neutron energies between 4 and 40 MeV were fit to determine the (spherical) neutron potential. A comparison of calculated and measured[32] total, elastic, and nonelastic cross sections from 12 to 80 MeV is given in Fig. 13. Agreement is seen to be very good below 40 MeV, where the fitting was done. Neutron transmission coefficients for this analysis, together with proton and alpha transmission coefficients, gamma-ray strength functions, level density parameters, and preequilibrium parameters, were used to calculate all significant neutron, proton, alpha, and gamma-ray production cross sections to 40 MeV.

Analyses similar to the ^{40}Ca study have been performed to 40 MeV for ^{54,56}Fe (Ref. 25) and to 50 MeV for ^{59}Co (Ref. 26) using the GNASH code. As was the case in the analyses discussed here, simple forms were found for the neutron and charged-particle potentials that described the reactions from very low energies to the maximum energies of the analyses.

New Developments In Spectrum Calculations

Two other developments in the application of theory for data evaluation should be mentioned. The first of these involves calculations of beta decay properties, specifically, decay spectra and half-lives. Mann et al[87] have found that by multiplying the level density parameter, a, by the ratio N/(N+Z), where N and Z are the numbers of neutrons and protons in the daughter nucleus, simple statistical theory can be used to calculate average beta decay spectra and half-lives. Using a microscopic approach, Klapdor et al[88] have reproduced measured structure in more detailed calculations of beta spectra. Both methods appear more promising than the gross theory of beta decay,[89] as is illustrated by the comparison of measured and calculated half-lives for Rb isotopes in Fig. 14.

A second development in spectral calculations is the recent work of Madland and Nix,[90] which uses standard nuclear evaporation theory to calculate both the average number of neutrons ($\bar{\nu}_p$) and neutron spectra [N(E)] from prompt fission. The calculations include the effects of first-, second-, and third-chance fission. It is shown that, using certain well-measured fission-related quantities, $\bar{\nu}_p$ and N(E) can be reliably predicted. Improvements in this technique and its application to spontaneous fission of ^{252}Cf are the subject of another paper at this conference.[91]

Conclusions

It is evident that the present generation of nuclear theory and model codes used for data evaluation has

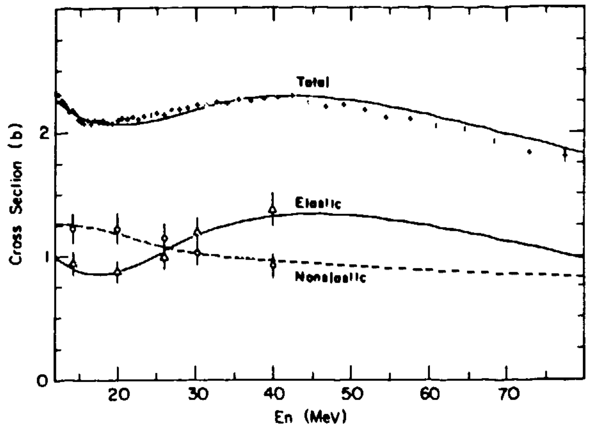

ig. 13. The optic. . model analysis of Ref. 83 com- ɜred to measurements[32] of n + ^{40}Ca total, elastic, ıd non-elastic cross sections.

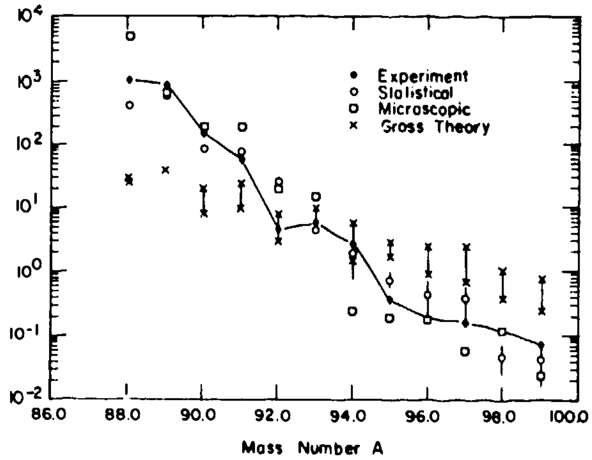

ig. 14. Comparison of measured and calcu'ated half- ives for Rb isotopes over the range A = 88-99.

ɜen quite successful in describing a variety of nu- lear reaction data. Substantial progress has been ɜde in several areas of applied theory, particularly ı developing techniques for determining nuclear model ɜrameters. There remains, however, a number of areas ıere improvements are needed in the models, particu- ɹrly if reliable extrapolations to regions away rom measured data.

ı several of the analyses that were described, calcu- ɜtions were performed to energies considerably above) MeV. For example, a composite of reaction cross ɜctions from the n + ^{59}Co analysis[26] to 50 MeV is ıown in Fig. 15. For this analysis, no experimental ɜta on these reactions were available above 24 MeV ıd only limited data from 8-13 and 15-24 MeV. The ivision of the nonelastic cross section into the var- ɔus reaction channels, together with calculation of nission energy spectra and angular distributions, was ccomplished entirely with the simple models described ɔove. Here we are not only depending on reliable es- imates of energy dependence in the models, we are al- ɔ assuming their accuracy as we drift off the line of tability. Clearly, improved methods are required for ɔnfidence in calculations such as these.

f the topics covered in this review, level density ɔrmulation probably constitutes the area most in need f improvement. A good deal of the theoretical basis

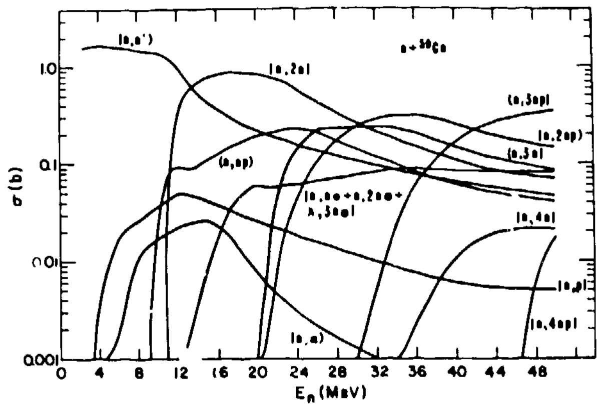

Fig. 15. Calculated[26] reaction cross sections for n + ^{59}Co interactions to 50 MeV.

for such improvements already exists, but implementation of more detailed microscopic theories without overly complicating applied calculations has been an obstacle.

Reliable optical model analyses are obviously essential for applied calculations and continued improvement in methods and actual parameterizations is important. While significant progress has been made in developing neutron and proton potentials, relatively little advance has occurred for alpha particle potentials, and improvement is needed for reliable calculations of helium production. From the point of view of data prediction, greater use of microscopic optical model calculations should facilitate more meaningful extrapolations into unmeasured regions.

Preequilibrium models have been highly successful in calculating particle emission spectra near 14 MeV. How well such models do in describing the dependence of spectra on incident energy is less well established and further development is certainly required for angular distribution effects. Continued advance of unified reaction theories is particulary important for higher energies and should put the entire calculational framework on a sounder theoretical footing.

Finally, although not covered in this review, fission theory remains an area much in need of improvement if reliable predictions of data are to be realized in the actinide region.

References

1. E. D. Arthur, "Calculational Methods Used to Obtain Evaluated Data above 3 MeV," Proc. Conf. on Nuclear Data Evaluation Methods and Procedures, Brookhaven, Sept. 22-25, 1980 (BNL-NCS-51363, 1981) p. 655.

2. Ch. Lagrange, "Comments on Some Aspects of the Use of Optical Statistical Models for Evaluations," ibid, p. 59C

3. D. G. Gardner, "Current Status of Fast Neutron Capture Calculations," to be published in Proc. NEANDC/NEACRP Specialists Meeting on Fast-Neutron Capture Cross Sections, Argonne, April 20-23, 1982.

4. P. A. Moldauer, "Statistical Applications of Neutron Nuclear Reactions," Proc. of Course on Nuclear Theory for Applications, Trieste, Jan. 17-Feb. 10, 1978 (IAEA-SMR-43, 1980) p. 165.

5. C. Mahaux, "Theoretical Aspects of the Optical Model," ibid, p. 97.

6. F. Gadioli and E. Gadioli Errba, "Recent Results in the Theoretical Description of Preequilibrium Processes," Proc. Course on Nuclear Theory for Applications, Trieste, Jan. 28-Feb. 22, 2980 (IAEA-SMR-68/I) p. 3. For example, H. John, "Absolute values of Inelastic Neutron Scattering with Account Taken of the Preequilibrium Mechanism, ibid, p. 293.

7. E. D. Arthur, "Use of the Statistical Model for the Calculation of Compound Nucleus Contributions to Inelastic Scattering on Actinide Nuclei," Proc. Specialists Meeting on Fast Neutron Scattering on Actinide Nuclei, Paris, Nov. 23-25, 1981 (NEANDC-158U, 1982) p. 145.

8. G. M. Hale, "R-Matrix Analysis of the ^{7}Li System," Proc. Conf. on Neutron Standards and Applications, Wash., D. C., Mar. 28-31, 1977 (NBS Spec. Publ. 493, (1977) p. 30.

9. G. M. Hale, "R-Matrix Analysis of the Light Element Standards," Proc. Conf. Nuclear Cross Sections and Tech., Wash., D.C., Mar. 3-7, 1975 (NBS Spec. Publ. 425, 1975) p. 302.

10. P. G. Young, "Summary Documentation of Nuclear Data Evaluations for ENDF/B-V," LA-7663-MS (1979).

11. G. M. Hale, "Calculations of Neutron Spectra from the n + d Reaction," in "Applied Nuclear Data Research and Development, July 1 - Sept. 30, 1981," LA-9262-PR (1982) p. 1.

12. M. Brüllmann et al, Nucl. Phys. A117, 419 (1968); S. Messelt, ibid, 48, 512 (1963).

23. R. M. Frank and J. L. Gammel, Phys. Rev. 93, 463 (1954); Yu. I. Chernuklin and R. S. Shuvalov, J. Nucl. Phys. (USSR) 4, 197 (1967).

14. P. G. Young, Trans. Am. Nucl. Soc. 39, 272 (1981).

15. R. E. Prael, Trans. Am. Nucl. Soc. 41, 480 (1982).

16. C. A. Engelbrecht and H. A. Weidenmüller, Phys. Rev. C8, 859 (1973).

17. H. Feshbach et al, Ann. Phys. (NY) 125, 429 (1980).

18. T. Tamura et al, Phys. Rev. C23, 2769 (1981).

19. E. Sheldon and D. W. S. Chan, "Evaluation of (n,n') Scattering Cross Sections from 0.8 to 2.5 MeV for Higher Collective Bands of ^{232}Th and ^{238}U in 'Standard' (CN + DI) and 'Unified' (Weidenmuller S-Matrix) Formalisms," Proc. Specialists Mtg. on Fast Neutron Scattering on Actinide Nuclei, Paris, Nov. 23-25. 1981 (NEANDC-158U, 1982) p. 169.

20. R. Bonetti et al, Phys. Rev. C24, 71 (1981).

21. H. A. Weidenmüller, "Beyond the Statistical Model: Recent Progress in Neutron Nuclear Reaction Theory," Proc. Conf. Nuclear Data for Science and Tech., Antwerp, Sept. 6-10, 1982, to be issued.

22. E. Sheldon, "Level Excitation Function Data for Fast Neutron Scattering on Actinide Nuclei Calculated with the Unified Statistical S-Matrix Formalism," ibid.

23. J. P. Delaroche et al, "The Optical Model with Particular Considerations of the Coupled-Channel Optical Model," IAEA-190 (1976), p. 251.

24. E. D. Arthur, Nucl. Sci. Eng. 76, 137 (1980).

25. E. D. Arthur and P. G. Young, "Evaluation of Neutron Cross Sections to 40 MeV for ^{54,56}Fe," Proc. Symp. Neutron Cross Sections from 10-50 MeV, Brookhaven, May 12-14, 1980 (BNL-NCS-51245, 1980), p. 731.

26. E. D. Arthur et al, "Calculation of ^{59}Co Neutron Cross Sections Between 3 and 50 MeV," ibid, p. 751.

27. Ch. Lagrange et al, to be published in Nucl. Sci. Eng. (1982).

28. P. E. Hodgson, "The Neutron Optical Model in the Actinide Region," Proc. Specialists Mtg. on Fast Neutron Scattering on Actinide Nuclei, Paris, Nov. 23-25, 1981 (NEANDC-158U, 1982) p. 69.

29. A. M. Lane, Phys. Rev. Lett. 8, 171 (1962); A. M. Lane, Nucl. Phys. 35, 676 (1962).

30. J. Rapaport, Phys. Reports, in press (1982).

31. L. F. Hansen, "Study of Proton-Induced Reactions and Correlation with Fast Neutron Scattering," Proc. Specialists Mtg. on Fast Neutron Scattering on Actinide Nuclei, Paris, Nov. 23-25, 1981 (NEANDC-158U, 1982), p. 116.

32. D. I. Garber and R. R. Kinsey, "Neutron Cross Sections, Volume II, Curves," Brookhaven Natl. Lab. report BNL 325, 3rd Ed., Vol. 2 (1976), and personal communication from NNDC (1981).

33. S. D. Schery et al, Nucl. Phys. A234, 109 (1974).

34. L. F. Hansen et al, Bull. Am. Phys. Soc. 25, 728 (1980); L. F. Hansen et al, UCID-18987 (1981).

35. J. Rapaport et al., Nucl. Phys. A330, 15 (1979).

36. J. P. Jeukenne et al, Phys. Rev C16, 80 (1977).

37. Ch. Lagrange and J. C. Brient, "Interpretation Semi Microscopic de la Diffusion Elastique et Inelastique de Nucleons par ^{208}Pb," submitted to J. de Physique, Paris (1982).

38. F. S. Dietrich et al, Bull. Am. Phys. Soc. 27, 543 (1982).

39. J. M. Blatt and V. F. Weisskopf, Theoretical Nuclear Physics (John Wiley, New York, 1952) p. 627.

40. D. M. Brink, Thesis, Oxford University (1955) unpublished; P. Axel, Phys. Rev. 126, 671 (1962).

41. D. G. Gardner and F. S. Dietrich, "A New Parameterization of the E1 Gamma-Ray Strength Function," Conf. Nuclear Cross Sections for Tech., Knoxville, Oct. 22-26, 1979 (NBS Spec. Publ. 594, 1980) p 770; M. A. Gardner and D. G. Gardner, "Continued Study of the Parameterization of the E1 Gamma-Ray Strength Function," Symp. Neutron-Capture Gamma-Ray Spectroscopy and Related Topics, Grenoble, Sept. 7-11, 1981 (UCRL-86265).

42. G. Szeflinska et al, Nucl. Phys. A323, 253 (1979).

43. D. G. Gardner et al, "A Study of Gamma-Ray Strength Functions," UCID-18759 (1980).

44. W. Hauser and H. Feshbach, Phys. Rev. 87, 366 (1952).

45. A. Gilbert and A. G. W. Cameron, Can. J. Phys. 43, 1446 (1965).

46. W. Dilg et al, Nucl. Phys. A217, 269 (1973).

47. A. V. Ignatuyk et al, Sov. J. Nucl. Phys. 21, 255 (1975).

48. J. Jary and J. Frehaut, "Level Density Dependence of (n,γ), (n,n'), and (n,2n) Reaction Cross Sections," in Progress Report of the Neutron and Nuclear Physics Division for the year 1979, CEA-N-2134, p. 165 (1980).

49. G. Reffo, "Parameter Systematics for Statistical Theory Calculations of Neutron Reaction Cross Sections," CNEN-RT/FI-80 (1980).

50. J. L. Cook and E. K. Rose, "An Evaluation of the Gilbert-Cameron Level Density Parameters," AAEC/E419 (1977).

51. For example, J. R. Huizenga and L. G. Moretto, Ann. Rev. Nucl. Sci. 22, 427 (1972).

52. V. Benzi et al, Nuovo Cimento A66, 1 (1981); G. Maino et al, Nuovo Cimento A57, 427 (1980).

53. S. M. Grimes et al, Phys. Rev. C10, 2373 (1974).

54. J. L. Cook et al, Aust. J. Phys. 20, 477 (1967).

55. C. Kalbach, Acta. Phys. Slov. 25, 100 (1975).

56. M. Blann, Ann. Rev. Nucl. Sci. 25, 123 (1975).

57. J. M. Akkermans et al, Phys. Rev. C22, 73 (1980).

58. C. Kalbach and F. M. Mann, Phys. Rev. C23, 112 (1981).

59. J. M. Akkermans and H. Gruppelaar, Z. Phys. A300, 345 (1981).

60. C. Y. Fu, A Constant Nuclear Model for Compound and Precompound Reactions with Conservation of Angular Momentum," Oak Ridge report ORNL/TM 7042 (1980).

61. C. Y. Fu, "Summary of ENDF/B-V Evaluations for Carbon, Calcium, Iron, Copper, and Lead and ENDF/B-V Revision 2 for Calcium and Iron," Oak Ridge report ORNL/TM-8283 (1982).

62. P. G. Young, "Nuclear Model Codes and Data Evaluation," Proc. Symp. Neutron Cross Sections from 10 to 50 MeV, Brookhaven, May 12-14, 1980 (BNL-NCS-51245, 1980) p. 43.

63. A. Prince, "Analysis of High-Energy Neutron Cross Sections for Fissile and Fertile Isotopes," Proc. Intl. Conf. Nuclear Data for Reactors, IAEA (1970) p. 825.

64. P. G. Young and E. D. Arthur, "GNASH: A Preequilibrium Statistical Nuclear Model Code for Calculations of Cross Sections and Emission Spectra, Los Alamos report LA-6947 (1977).

65. F. M. Mann, "HAUSER-4: A Computer Code to Calculate Nuclear Cross Sections," Hanford report HEDL-TME-76-80 (1976).

66. B. Strohmaier and M. Uhl, "STAPRE - A Statistical Model Code with Consideration of Pre-Equilibrium Decay," Proc. Nuclear Theory for Applications, IAEA-SMR-43, p. 313 (1980).

67. C. Y. Fu, "Development of a Two-Step Hauser-Feshbach Code with Precompound Decays and Gamma-Ray Cascades," Proc. Nuclear Cross Sections and Technolgy Conf., NBS Spec. Publ. 425 (1975), p. 328 .

68. C. L. Dunford, "A Unified Model for Analysis of Compound Nucleus Reactions," Atomics International report AI-AEC-12931 (1970).

69. D. G. Gardner, "Recent Developments in Nuclear Reaction Theories and Calculations," Proc. Symp. Neutron Cross Sections from 10 to 50 MeV, Brookhaven, May 12-14, 1980 (BNL-NCS-51245, 1981) p. 641.

70. J. Jary, "MSPQ: A FORTRAN Code for Cross Section Calculations Using a Statistical Model with Pre-equilibrium Effects," INDC(FR)10L (1977).

71. M. Blann, "Overlaid ALICE,"University of Rochester report COO-3494-29 (1975).

72. O. Bersillon and L. Faugere, AMALTHEE: A Code for Spectra and Cross Section Calculations within the Exciton Model," NEANDC(D)191L (1977).

73. J. M. Akkermans and H. Gruppelaar, "Calculation of Preequilibrium Angular Distributions with the Exciton Model," ECN-60 (1979).

74. P. G. Young et al, "Analysis of n + ^{165}Ho and ^{169}Tm Reactions," Proc. Conf. Nuclear Data for Science and Technology, Antwerp, Sept. 6-10, 1982 to be issued.

75. E. D. Arthur and C. A. Philis, "Calculations of Neutron Cross Sections for Tungsten Isotopes," Proc. Conf. Nuclear Cross Sections for Technology, Knoxville, Oct. 22-26, 1979 (NBS Spec. Publ. 594, 1980), p. 333.

76. E. D. Arthur et al, Trans. Am. Nucl. Soc. 39, 793 (1981).

77. P. A. Moldauer, Nucl. Phys. 47, 65 (1963).

78. J. P. Delaroche et al, Phys. Rev. C23, 136 (1981).

79. A. B. Smith and P. T. Guenther, "On Neutron Inelastic-Scattering Cross Sections of ^{232}Th, ^{233}U, ^{235}U, ^{239}Pu, and ^{240}Pu," Argonne report ANL/NDM-63 (1982).

80. G. Haouat and Y. Patin, personal communication (1982).

81. B. Strohmaier and M. Uhl, "Nuclear Model Calculations of Neutron-Induced Cross Sections for ^{52}Cr, ^{55}Mn, ^{56}Fe, and ^{58,60}Ni for Incident Energies Up To 30 MeV," Proc. Conf. Nuclear Data for Science and Technology, Antwerp, Sept. 6-10, 1982, to be issued.

82. O. Bersillon et al, "A New Evaluation of Neutron Data for ^{209}Bi Between 10^{-5} eV and 20 Mev, ibid.

83. D. M. Hetrick et al, "Evaluated Neutron Induced Cross Sections for ^{209}Bi between 10^{-5} eV and 20 MeV," Oak Ridge report ORNL/TM-8290 (1982).

84. R. C. Haight and S. M. Grimes, UCRL-80235 (1977); S. M. Grimes, Phys. Rev. C19, 2127 (1979).

85. P. G. Young et al, "Application of Nuclear Models," Proc. Conf. Nuclear Cross Sections for Technology, Knoxville, Oct. 22-26, 1979 (NBS Spec. Publ. 594, 1980) p. 639.

86. G. T. Chapman et al, "A Re-Measurement of the Neutron-Induced Gamma-Ray Production Cross Sections for Iron in the Energy Range 850 keV $\le E_n \le$ 20.0 MeV," Oak Ridge report ORNL/TM-5416 (1976).

87. F. M. Mann et al, Phys. Rev. C25, 524 (1982).

88. H. V. Klapdor et al, Z. Phys. A299, 213 (1981).

89. K. Takahashi et al, At. Nucl. Data Tables 12, 101 (1973).

90. D. G. Madland and J. R. Nix, Nucl. Sci. Eng. 81, 213 (1982).

91. D. G. Madland and J. R. Nix, "Calculation of the Prompt Neutron Spectrum and Average Prompt Neuton Multiplicity for the Spontaneous Fission of ^{252}Cf," Proc. Conf. Nuclear Data for Science and Technology, Antwerp, Sept. 6-10, 1982, to be issued.